

Féry IR Spectrometer for Single-Shot Analysis of Protein Dynamics

Eglof Ritter^{†,|,}, Ljiljana Puskar[‡], So Young Kim[§], Jung Hee Park[§], Klaus Peter Hofmann[¶], Franz Bartl[|], Peter Hegemann[†], and Ulrich Schade[‡].*

[†]Humboldt-Universität zu Berlin, Experimentelle Biophysik, 10115 Berlin, Germany

[‡]Helmholtz-Zentrum Berlin für Materialien und Energie, 12498 Berlin, Germany

[§]Chonbuk National University, Division of Biotechnology, Advanced Institute of Environment and Bioscience, 54596 Iksan, Republic of Korea

[¶]Charité – Universitätsmedizin Berlin, 10117 Berlin, Germany

[|]Humboldt-Universität zu Berlin, Biophysikalische Chemie, 10115 Berlin.

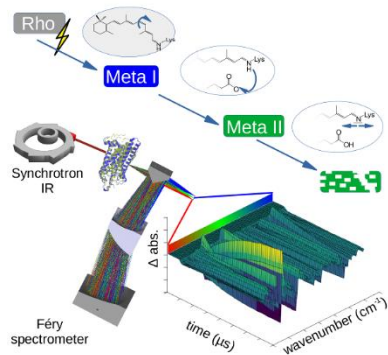
AUTHOR INFORMATION

Corresponding Author

[*eglof.ritter@hu-berlin.de](mailto:eglof.ritter@hu-berlin.de)

ABSTRACT. Current sub-millisecond time-resolved broadband infrared spectroscopy, one of the most frequently used techniques to study structure-function relationships in life sciences, is typically limited to fast-cycling reactions that can be repeated thousands of times with high frequency. Notably, the majority of chemical and biological processes do not comply with this requirement. For example, the activation of vertebrate rhodopsin, prototype of many protein receptors in biological organisms that mediate basic functions of life including vision, smell, and taste, is irreversible. Here we present a dispersive single-shot Féry spectrometer setup that extends such spectroscopy to irreversible and slow-cycling systems by exploiting the unique properties of brilliant synchrotron infrared light combined with an advanced focal-plane detector array embedded in a dispersive optical concept. We demonstrate our single-shot method on microbial actinorhodopsin with a slow photocycle, and on vertebrate rhodopsin with irreversible activation.

TOC GRAPHICS



KEYWORDS: Infrared Spectroscopy, Single-Shot, Time-Resolved Spectroscopy, FTIR, Synchrotron Infrared.

Vertebrate rhodopsin is the initiating protein in the visual cascade that converts light into a neuronal signal. Importantly, rhodopsin is the prototype of G-protein coupled receptors (GPCR), a large receptor family that consists of more than 1000 individual members including the cannabinoid receptor, the β -adrenergic receptor, hormone receptors, and many others¹. Approximately 34 % of all marketed drugs target the GPCR family², and rhodopsin is the key model for studying conserved GPCR functions and dynamics. Light absorption and isomerization of the retinal chromophore in rhodopsin triggers a stepwise transformation from an inactive (dark) state into an active (signaling) state at a timescale that ranges from nanoseconds to milliseconds.

Among protein characterization techniques, IR spectroscopy is commonly used to monitor both local and global changes in proteins including secondary structure³, the retinal cofactor⁴, amino acid side chains⁵, lipid ester head-groups⁶, and proton transport and hydrogen bonded network dynamics⁷. More specifically, Fourier transform IR (FTIR) difference spectroscopy has become the standard method because it detects changes in individual bonds and groups and distinguishes them among thousands of vibrations that occur in a complex protein^{4,5}. However, to date, an in-depth time-resolved study of the rhodopsin activation cascade using established FTIR methods has not been possible due to the requirement that sub-millisecond time-resolved FTIR must be applied to cyclic samples where the exact same reaction path can be triggered more than a thousand times in rapid succession. This limitation arises from the basic principle of the standard FTIR step-scan technique that is used for events that occur at sub-millisecond time-scales (reviewed by Ritter et al.⁸). Vertebrate rhodopsin is non-cyclic and bleaches irreversibly after photon absorption; therefore, experimental repetition with the same sample is not feasible⁹. Consequently, the rhodopsin reaction cascade has to be measured in a

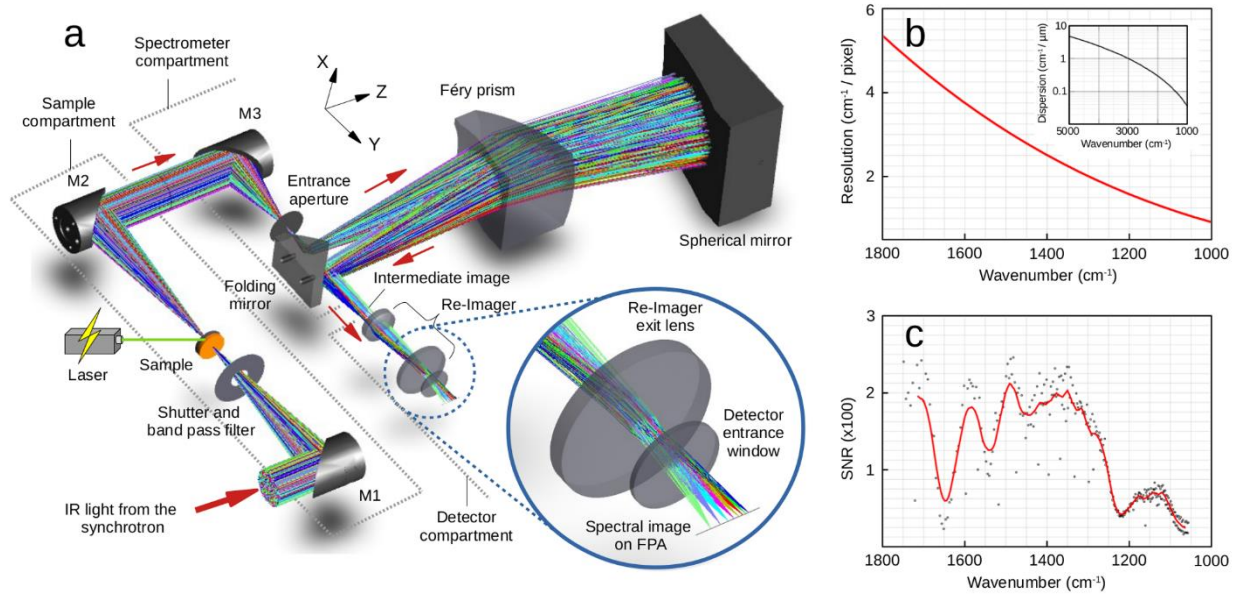


Figure 1. (a) Optical layout of the Féry spectrometer with the beam path shown between 1800 cm^{-1} (blue lines) and 1000 cm^{-1} (green lines). Inset: The spectral image on the FPA pixel detector. (b) The spectral resolution as a function of the wavenumber in the range of interest. Inset: The wavelength dependent dispersion, in units of $\text{cm}^{-1}/\mu\text{m}$, over a broader spectral range. (c) The measured signal to noise ratio (SNR) relevant for the protein difference spectra as a function of the wavenumber.

single-shot mode, where successive spectra are acquired as a function of time from a single turnover experiment. For cyclic systems, including several microbial rhodopsins, this FTIR limitation has substantial consequences when a reaction cycle comprises one or more slow reaction steps. In these circumstances, long recovery times between individual experiments are necessary, and low repetition frequency prevails. This leads to measurements that demand high protein stability and robust instrumentation, in addition to extremely long experiment times. For example, to analyze a full photocycle of the widely applied optogenetic actuator channelrhodopsin¹⁰, weeks of data acquisition are required using the step-scan FTIR technique^{11–13}.

In FTIR-based true single-shot methods (rapid-scan FTIR), the spectral acquisition speed is mechanically limited by a moving element. Although reducing the moving element path length allowed to increase the time-resolution into the microsecond time scale down to $13\text{ }\mu\text{s}^{14}$, it is inversely related to the spectral resolution¹⁵. Monochromatic quantum cascade lasers have been employed to overcome the FTIR limitation, but the acquisition of spectra requires multiple repetitions of the experiment, to account for the required spectral range and resolution¹⁶. In another recent study, quantum cascade laser optical frequency combs¹⁷ were employed to record spectra covering up to 55 cm^{-1} with a time resolution down to $0.3\text{ }\mu\text{s}^{18}$. Here, the spectral width and the signal to noise ratio (SNR) were limited by the availability of suitable lasers.

Our spectrometer design capitalizes on (i) an advanced focal plane detector array, (ii) the high brilliance of synchrotron infrared light, combined with (iii) a unique, diffraction limited dispersive optical setup¹⁹ (Figure 1a). Depending on the detector operation mode, it allows to record broad band spectra with time-resolutions down to $10\text{ }\mu\text{s}$. Whereas conventional FTIR spectrometers benefit from high throughput by using large entrance apertures, in a dispersive instrument, small entrance apertures must be used to ensure spectral resolution. Furthermore, FTIR spectrometers have a multiplex advantage where all wavelength intervals and thus the total light intensity contributes to the signal at the single detector element, while in a dispersive device only a small fraction of the diffracted light corresponding to a single wavelength interval reaches a given detector element. This throughput and multiplex advantages are one of the primary reasons why to date predominantly Fourier transform spectrometers have been employed for vibrational spectroscopy¹⁵.

In our dispersive set-up, brilliant synchrotron IR light allows for orders of magnitude higher light energy to be used with micrometer scale entrance apertures²⁰. The core of the spectrometer

comprises an IR-transparent prism (Féry prism) with two spherical surfaces²¹ and a spherical mirror that is positioned behind the prism such that light from the entrance aperture passes through the prism twice²². The implementation of a prism rather than a conventional grating avoids both order effects and stray light, and consequently, ensures optimal utilization of the available photon flux. Image formation by the spectrometer follows aplanatic principles²³ to produce a flat spectral image of the entrance aperture that is aligned with the detector pixel line and ensures that the maximum light energy reaches the individual detector elements (see SI Figure S1, SI Note S1, and SI Note S4).

The spectrometer was built at the IRIS beamline of the electron synchrotron BESSY II facility (SI Figure S2). We confirmed the spectral resolution (Figure 1b) and wavelength calibration by comparing the emission spectrum of a quantum cascade laser and the absorbance spectrum of a polystyrene reference standard with spectra of the same samples that were obtained with a conventional FTIR spectrometer (SI Figure S4). When protein conformational changes are studied, difference spectra are recorded that only reflect the changes in the protein induced by an external perturbation. Such spectral changes are in the order of 10^{-2} - 10^{-3} compared to the total absorbance^{5,8} and accordingly demand for a high signal to noise ratio (SNR). The SNR that is relevant to the protein difference spectra was estimated individually for each detector pixel from the fluctuations in time with a protein sample in place, with 30 μ s time resolution. The SNR as a function of the wavelength interval (SNR spectrum) is presented in Figure 1c (for a SNR spectrum in absorbance mode, see SI Figure S3). High SNR values between 50 and 200 indicated that protein conformational changes could be studied with our IR difference spectrometer in single-shot mode.

We applied our spectrometer to characterize two photoreceptor proteins: (1) the recently discovered microbial actinorhodopsin²⁴ that has a moderately slow photocycle, and (2) non-cyclic

bovine rhodopsin. Both of these proteins are incompatible with the step-scan technique because it is either time-consuming or impossible to apply, respectively. We studied both proteins with a time resolution of 30 μ s.

The interest in microbial rhodopsins has increased in recent years because of expanding applications in the field of optogenetics¹⁰. Actinorhodopsins from planktonic actinobacteria are unusual light-driven outward proton pumps²⁴. In nature, they have an important role in energy circulation within freshwater ecosystems²⁵. The binding pocket of these proteins can accommodate carotenoids in addition to the retinal chromophore, which provide a potent light-harvesting antenna similar to xanthorhodopsins²⁶. This dual chromophore²⁷ present in actinorhodopsins doubles the light-harvesting efficiency²⁸. In addition, the dual chromophore can efficiently tune or broaden the optical absorbance maximum, which could turn the protein into an interesting candidate for optogenetic applications. Photon absorption in the retinal chromophore causes all-*trans* to 13-*cis* isomerization, which triggers a photocycle (Figure 2a) that has a total cycling time of ~100 ms. One of the decisive proton transfer steps as identified from UV-Vis spectroscopy²⁹ is deprotonation of the Schiff base C=N bond that connects the protein to the chromophore and leads to a blue-shifted visible absorption state (M state). The Schiff base is then reprotonated when the M state transitions into the next intermediate (Figure 2a). However, the mechanistic basis of these processes remains largely unknown, and to our knowledge, no IR spectra have been reported. We followed the photocycle of wild type (Figure 2b, c, and e) and mutant E103Q actinorhodopsin (Figure 2d and f). In the mutant photoreceptor, the putative proton donor to the Schiff base was neutralized, which slowed down the late photocycle reaction.

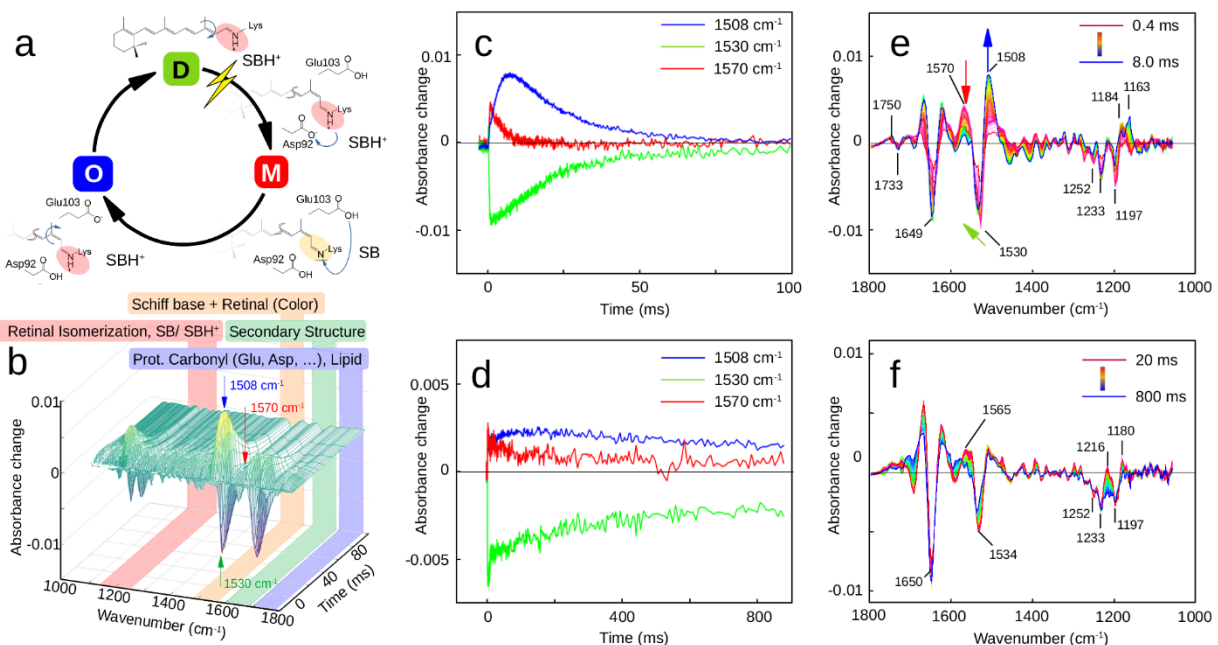


Figure 2. Infrared difference spectroscopy of actinorhodopsin. (a) Photocycle model of actinorhodopsin with the dark state D, state with deprotonated Schiff base M, and a late intermediate O. (b) Time-resolved infrared difference spectra of the wild-type actinorhodopsin with spectral regions-of-interest marked. (c) Light-triggered kinetics of the infrared bands representing formation and decay of photocycle intermediates (red: M, blue: O, green: D). (d) Kinetics of the same bands of the mutant E103Q. (e) Infrared difference spectra of the wild-type (0.4 - 8 ms), corresponding to the M to O conversion. (f) Difference spectra of the mutant E103Q (20 - 800 ms).

The isolated kinetics of the band at 1570 cm^{-1} were indicative of the M state and the kinetics at 1508 cm^{-1} were indicative of a later intermediate. The kinetics was slowed down by an order of magnitude in the mutant. Our data present the first continuous decay kinetics of this specific microbial rhodopsin. In addition, the data allowed us to isolate the spectral signatures of both the M state and the late O state. The latter can be identified as the red-shifted species known as P620²⁹. The band at 1733 cm^{-1} can be assigned to the C=O mode of protonated E103. The data confirmed E103 as the proton donor of the Schiff base and showed that its neutralization prolonged the

lifetime of the M state by more than an order of magnitude under low humidity condition (for details and band assignments, see SI Note S2). The spectral fingerprints of the M and O states are represented as red and blue lines in Figure 2e,f, respectively. The total measurement time was approximately 20 min to account for recovery of the mutant with a minimum regeneration time of 20 s (64 experiment repetitions). Notably, a comparable step-scan experiment (spectral resolution of 4.5 cm^{-1}) would require more than half a day of data acquisition to achieve similar spectral quality (details in the SI Note S4).

To apply our spectrometry approach to a true non-cyclic system, we investigated bovine rhodopsin, which is responsible for vision in dim light conditions. This type of irreversible photoreaction is impossible to study with the conventional step-scan FTIR technique. Photoactivation of bovine rhodopsin triggers conformational dynamics of the protein moiety that leads via an early Lumi intermediate to an equilibrium between inactive Metarhodopsin (Meta) I and the active state, Meta II³⁰. The latter state decays irreversibly by Schiff base hydrolysis, and retinal release occurs within minutes (Figure 3a). The crucial step in this process is the transformation from the Meta I to the Meta II state, which requires deprotonation of the Schiff base and important structural rearrangements including helix elongation and movement that facilitate G-protein binding pocket formation on the millisecond timescale (Figure 3b). Although IR spectroscopy has been widely used to investigate rhodopsin activation, to date, the intermediates have only been studied by IR in cryotrapped states due to the photoconversion irreversibility. Our setup enabled us to measure the conversion dynamics of the Lumi, Meta I, and Meta II states of bovine rhodopsin from a

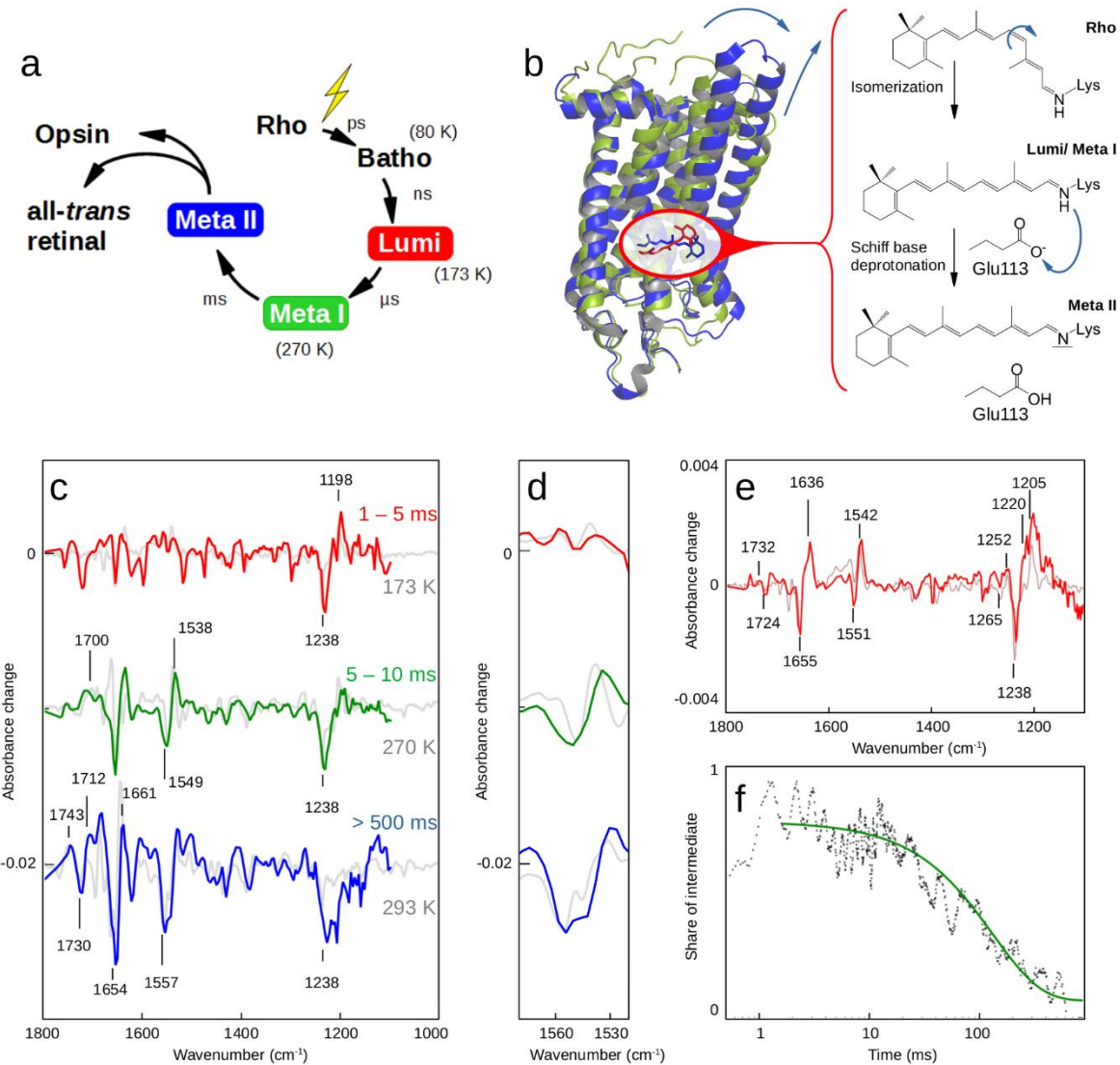


Figure 3. The irreversible photoreaction of vertebrate rhodopsin. (a) Schematic of the rhodopsin activation cascade beginning from the dark state (Rho) towards Meta II and Schiff base hydrolysis, with temperatures for cryotrapping indicated. (b) Schematic of Rho (green) and Meta II (blue) structures with retinal isomerization and proton transfers (inset). (c) Time-resolved infrared difference spectra showing Lumi (red, $\sim 1\text{--}5 \text{ ms}$), Meta I (green, $\sim 5\text{--}10 \text{ ms}$), and Meta II (blue, $>500 \text{ ms}$), and corresponding cryotrapped intermediates (grey). Data were obtained by averaging the single-shot measurements from 7 samples. (d) Amide II region of the same spectra to identify the intermediates. (e) Extraction of the improved Lumi spectrum by SVD and global analysis. (f) Decay kinetics of Meta I (half-life of $\tau_{1/2} \sim 90 \text{ ms}$).

time-resolved continuous data set in real-time (Figure 3c). Importantly, the spectra exhibited the typical known patterns for the temperature-stabilized intermediates⁴. For example, the isomerization of retinal from 11-*cis* to all-*trans* was represented by a negative band at 1238 cm⁻¹. A positive mode at 1198 cm⁻¹ in the first and second observed intermediates corresponded to the Lumi and Meta I states. Schiff base deprotonation upon formation of the Meta II state (Figure 3b) was indicated by the complete disappearance of the mode around 1198 cm⁻¹ from the second to the third spectrum (Figure 3c). Note that systematic error signals introduced by the laser flash and source oscillations are still seen in the raw spectrum of Lumi (Figure 3c). However, the amide II region around 1550 cm⁻¹ is highly sensitive to changes of the chromophore and the protein and thus confirms the formation of Lumi (Figure 3d). An improved difference spectrum of the Lumi intermediate was achieved through singular value decomposition combined with global fitting analysis (Figure 3e), a standard method also used for rapid-scan or step-scan FTIR. Through this procedure, corresponding kinetics of all intermediates were also obtained with the example of Meta I shown in Fig. 3f. Additional details on this procedure and details related to the time-resolved infrared spectra of rhodopsin are given in SI Note S3.

In conclusion, our novel approach employs microsecond time-resolved IR spectroscopy to analyze irreversible reactions and significantly shortens the measuring time required for reversible, cyclic reactions that cannot be repeated on a timescale of seconds or faster. The current set up utilizes the brilliance of infrared synchrotron light, however with bright IR laser sources undergoing fast development and becoming more broadband^{31,32}, one can expect this method quickly extending beyond the large synchrotron facilities to the application in laboratory practice. Our technique paves the way for the application of single-shot IR spectroscopy to a broad range of biochemical reactions, including those that are naturally triggered by light or by the un-caging of bioactive

compounds. In addition, emerging applications for single-shot IR spectroscopy are present in fields outside of biochemistry where non-cyclic chemical reactions are studied, for example, water oxidation or catalytic systems research.

ASSOCIATED CONTENT

Supporting Information.

Additional Figures, Characterizations, and Experimental Section (PDF)

AUTHOR INFORMATION

Corresponding author: eglof.ritter@hu-berlin.de

Notes

The authors declare no competing financial interests.

ACKNOWLEDGMENT

We thank Kerstin Kalus, Klaus Ludwig, and Lars Ziemann for technical support and Patrick Piwowarski for discussion. We thank the Helmholtz-Zentrum Berlin (HZB) for providing synchrotron radiation beamtime. This work was supported by the German Federal Ministry of Education and Research (BMBF), Grant No. 05K16KH1, the Basic Science Research program through the National Research Foundation of Korea (NRF) funded by the Ministry of Science, ICT and Future Planning (NRF-2016R1D1A1B03934398), and the SFB (Sonderforschungsbereich) 1078 (to F.B. and P.H.).

REFERENCES

- (1) Hilger, D.; Masureel, M.; Kobilka, B. K. Structure and Dynamics of GPCR Signaling Complexes. *Nat. Struct. Mol. Biol.* **2018**, *25* (1), 4–12.
- (2) Hauser, A. S.; Chavali, S.; Masuho, I.; Jahn, L. J.; Martemyanov, K. A.; Gloriam, D. E.; Babu, M. M. Pharmacogenomics of GPCR Drug Targets. *Cell* **2018**, *172* (1–2), 41–54.
- (3) Yang, H.; Yang, S.; Kong, J.; Dong, A.; Yu, S. Obtaining Information about Protein Secondary Structures in Aqueous Solution Using Fourier Transform IR Spectroscopy. *Nat. Protoc.* **2015**, *10* (3), 382–396.
- (4) Siebert, F. Application of FTIR Spectroscopy to the Investigation of Dark Structures and Photoreactions of Visual Pigments. *Isr. J. Chem.* **1995**, *35* (3–4), 309–323.
- (5) Barth, A. Infrared Spectroscopy of Proteins. *Biochim. Biophys. Acta - Bioenerg.* **2007**, *1767* (9), 1073–1101.
- (6) Isele, J.; Sakmar, T. P.; Siebert, F. Rhodopsin Activation Affects the Environment of Specific Neighboring Phospholipids: An FTIR Spectroscopic Study. *Biophys. J.* **2000**, *79* (6), 3063–3071.
- (7) Zundel, G. Hydrogen Bonds with Large Proton Polarizability and Proton Transfer Processes in Electrochemistry and Biology. In *Advances in Chemical Physics*; **2007**; 1–217.
- (8) Ritter, E.; Puskar, L.; Bartl, F. J.; Aziz, E. F.; Hegemann, P.; Schade, U. Time-Resolved Infrared Spectroscopic Techniques as Applied to Channelrhodopsin. *Front. Mol. Biosci.*

2015, 2 (38).

- (9) Ebrey, T. G. The Thermal Decay of the Intermediates of Rhodopsin in Situ. *Vision Res.* **1968**, *8* (8), 965–982.
- (10) Deisseroth, K.; Hegemann, P. The Form and Function of Channelrhodopsin. *Science* **2017**, *357* (6356).
- (11) Lorenz-Fonfria, V. A.; Resler, T.; Krause, N.; Nack, M.; Gossing, M.; Fischer von Mollard, G.; Bamann, C.; Bamberg, E.; Schlesinger, R.; Heberle, J.; et al. Transient Protonation Changes in Channelrhodopsin-2 and Their Relevance to Channel Gating. *Proc. Natl. Acad. Sci. U. S. A.* **2013**, *110* (14), E1273-E1281.
- (12) Kuhne, J.; Eisenhauer, K.; Ritter, E.; Hegemann, P.; Gerwert, K.; Bartl, F. Early Formation of the Ion-Conducting Pore in Channelrhodopsin-2. *Angew. Chemie - Int. Ed.* **2015**, *54* (16), 4953–4957.
- (13) Kuhne, J.; Vierock, J.; Tennigkeit, S. A.; Dreier, M.-A.; Wietek, J.; Petersen, D.; Gavriljuk, K.; El-Mashtoly, S. F.; Hegemann, P.; Gerwert, K. Unifying Photocycle Model for Light Adaptation and Temporal Evolution of Cation Conductance in Channelrhodopsin-2. *Proc. Natl. Acad. Sci.* **2019**, *116* (19), 9380-9398
- (14) Süss, B.; Ringleb, F.; Heberle, J. New Ultrarapid-Scanning Interferometer for FT-IR Spectroscopy with Microsecond Time-Resolution. *Rev. Sci. Instrum.* **2016**, *87* (6), 063113.
- (15) Stuart, B. H. *Infrared Spectroscopy: Fundamentals and Applications; Analytical Techniques in the Sciences*; John Wiley & Sons, Ltd: Chichester, UK, 2004.

- (16) Lórenz-Fonfría, V. A.; Schultz, B. J.; Resler, T.; Schlesinger, R.; Bamann, C.; Bamberg, E.; Heberle, J. Pre-Gating Conformational Changes in the ChETA Variant of Channelrhodopsin-2 Monitored by Nanosecond IR Spectroscopy. *J. Am. Chem. Soc.* **2015**, *137* (5), 1850–1861.
- (17) Hugi, A.; Villares, G.; Blaser, S.; Liu, H. C.; Faist, J. Mid-Infrared Frequency Comb Based on a Quantum Cascade Laser. *Nature* **2012**, *492* (7428), 229–233.
- (18) Klocke, J. L.; Mangold, M.; Allmendinger, P.; Hugi, A.; Geiser, M.; Jouy, P.; Faist, J.; Kottke, T. Single-Shot Sub-Microsecond Mid-Infrared Spectroscopy on Protein Reactions with Quantum Cascade Laser Frequency Combs. *Anal. Chem.* **2018**, *90* (17), 10494–10500.
- (19) Schade, U.; Ritter, E.; Hegemann, P.; Aziz, E. F.; Hofmann, K. P. Concept for a Single-Shot Mid-Infrared Spectrometer Using Synchrotron Radiation. *Vib. Spectrosc.* **2014**, *75*, 190–195.
- (20) Schade, U.; Röseler, A.; Korte, E. H.; Bartl, F.; Hofmann, K. P.; Noll, T.; Peatman, W. B. New Infrared Spectroscopic Beamline at BESSY II. *Rev. Sci. Instrum.* **2002**, *73* (3), 1568–1570.
- (21) Féry, C. A Prism with Curved Faces, for Spectrograph or Spectroscope. *Astrophys. J.* **1911**, *34* (79).
- (22) Wilson, R. N. Die Anwendung von Aplanatischen Prismen in Monochromatoren Und Spektrographen. *Optik (Stuttg.)*. **1969**, *29* (1), 17–29.
- (23) Warren, D. W.; Hackwell, J. A.; Gutierrez, D. J. Compact Prism Spectrographs Based on

Aplanatic Principles. *Opt. Eng.* **1997**, *36* (4), 1174.

- (24) Sharma, A. K.; Zhaxybayeva, O.; Papke, R. T.; Doolittle, W. F. Actinorhodopsins: Proteorhodopsin-like Gene Sequences Found Predominantly in Non-Marine Environments. *Environ. Microbiol.* **2008**, *10* (4), 1039–1056.
- (25) Dwulit-Smith, J. R.; Hamilton, J. J.; Stevenson, D. M.; He, S.; Oyserman, B. O.; Moyano-Flores, F.; Garcia, S. L.; Amador-Noguez, D.; McMahon, K. D.; Forest, K. T. AcI Actinobacteria Assemble a Functional Actinorhodopsin with Natively Synthesized Retinal. *Appl. Environ. Microbiol.* **2018**, *84* (24).
- (26) Balashov, S. P.; Imasheva, E. S.; Boichenko, V. A.; Antón, J.; Wang, J. M.; Lanyi, J. K. Xanthorhodopsin: A Proton Pump with a Light-Harvesting Carotenoid Antenna. *Science* **2005**, *309* (5743), 2061–2064.
- (27) Luecke, H.; Schobert, B.; Stagno, J.; Imasheva, E. S.; Wang, J. M.; Balashov, S. P.; Lanyi, J. K. Crystallographic Structure of Xanthorhodopsin, the Light-Driven Proton Pump with a Dual Chromophore. *Proc. Natl. Acad. Sci.* **2008**, *105* (43), 16561–16565.
- (28) Imasheva, E. S.; Balashov, S. P.; Choi, A. R.; Jung, K.; Lanyi, J. K. Reconstitution of *Gloeobacter Violaceus* Rhodopsin with a Light-Harvesting Carotenoid Antenna. *Biochemistry* **2009**, *48* (46), 10948–10955.
- (29) Nakamura, S.; Kikukawa, T.; Tamogami, J.; Kamiya, M.; Aizawa, T.; Hahn, M. W.; Ihara, K.; Kamo, N.; Demura, M. Photochemical Characterization of Actinorhodopsin and Its Functional Existence in the Natural Host. *Biochim. Biophys. Acta - Bioenerg.* **2016**, *1857* (12), 1900–1908.

- (30) Hofmann, K. P.; Scheerer, P.; Hildebrand, P. W.; Choe, H. W.; Park, J. H.; Heck, M.; Ernst, O. P. A G Protein-Coupled Receptor at Work: The Rhodopsin Model. *Trends Biochem. Sci.* **2009**, *34* (11), 540–552.
- (31) Borondics, F.; Jossent, M.; Sandt, C.; Lavoute, L.; Gaponov, D.; Hideur, A.; Dumas, P.; Février, S. Supercontinuum-Based Fourier Transform Infrared Spectromicroscopy. *Optica* **2018**, *5* (4), 378.
- (32) Petersen, C. R.; Moselund, P. M.; Huot, L.; Hooper, L.; Bang, O. Towards a Table-Top Synchrotron Based on Supercontinuum Generation. *Infrared Phys. Technol.* **2018**, *91*, 182–186.